Published in final edited form as:
Neuron. 2013 March 20; 77(6): 1151–1162. doi:10.1016/j.neuron.2013.01.038.

Inhibition of medio-dorsal thalamus disrupts thalamo-frontal connectivity and cognition

S. Parnaudeau[1,2,*], **P.K. O'Neill**[1,*], **S. Bolkan**[1,2], **R.D. Ward**[1], **A.I. Abbas**[1,4], **B.L. Roth**[3], **P. Balsam**[1], **J.A. Gordon**[1,†], and **C. Kellendonk**[1,2,†]

[1]Department of Psychiatry, Columbia University, New York, NY10032 USA

[2]Department of Pharmacology, Columbia University, New York, NY10032 USA

[3]Department of Pharmacology, University of North Carolina at Chapel Hill School of Medicine, 4009 Genetics Medicine CB7365, Chapel Hill, NC 27599-7365 USA

[4]Department of Integrative Neuroscience, New York State Psychiatric Institute, New York, NY 10032 USA

SUMMARY

Cognitive deficits are central to schizophrenia but the underlying mechanisms still remain unclear. Imaging studies performed in patients point to decreased activity in the medio-dorsal thalamus (MD) and reduced functional connectivity between the MD and prefrontal cortex (PFC) as candidate mechanisms. However, a causal link is still missing. We used a pharmacogenetic approach in mice to diminish MD neuron activity and examined the behavioral and physiological consequences. We found that a subtle decrease in MD activity is sufficient to trigger selective impairments in prefrontal-dependent cognitive tasks. *In vivo* recordings in behaving animals revealed that MD-PFC beta-range synchrony is enhanced during acquisition and performance of a working memory task. Decreasing MD activity interfered with this task-dependent modulation of MD-PFC synchrony, which correlated with impaired working memory. These findings suggest that altered MD activity is sufficient to disrupt prefrontal-dependent cognitive behaviors, and could contribute to the cognitive symptoms observed in schizophrenia.

INTRODUCTION

Schizophrenia is a devastating mental disorder characterized by three clusters of symptoms: positive symptoms (psychosis and thought disorder), negative symptoms (social and emotional deficits) and cognitive symptoms. Understanding the cognitive symptoms of schizophrenia is of particular significance because they are highly predictive for the long-term prognosis of the disease and at present they are essentially resistant to treatment (Green, 1996). Cognitive symptoms include deficits in working memory and behavioral flexibility (Forbes et al., 2009; Leeson et al., 2009), two processes of executive function that are essential for activities of daily living. Functional magnetic resonance imaging studies have consistently shown an association between impaired executive function and altered

[†]To whom correspondence should be addressed. C. Kellendonk, ck491@columbia.edu and J.A.Gordon, jg343@columbia.edu.
[*]These authors contributed equally to this work.

activity in the prefrontal cortex (PFC) of patients, leading to the influential hypothesis that prefrontal dysfunction underlies the cognitive symptoms of schizophrenia (Weinberger and Berman, 1996). Due to its dense excitatory reciprocal connection with the PFC (Jones, 2007), the medio-dorsal thalamus (MD) has become a focus of attention in the study of cognitive symptoms. Imaging studies have repeatedly shown decreased activation of the MD in patients under a variety of test conditions that address executive functions (Andrews et al., 2006; Minzenberg et al., 2009). Altered correlation between activity in the MD and the PFC at rest or during cognitive testing has also been observed (Minzenberg et al., 2009; Mitelman et al., 2005; Woodward et al., 2012). These findings suggest that altered MD activity and/or impaired communication between the MD and PFC could play a role in the cognitive deficits seen in schizophrenia patients.

A major limitation of brain imaging studies is that they cannot draw causal relationships between measured physiological alterations and specific symptoms. As such, it remains unclear whether decreased MD activity is a cause or a consequence of schizophrenia and its associated cognitive dysfunction. Lesion studies in animal models have made a first step toward a better understanding of the roles of the PFC and the MD in executive function. While such studies clearly involved the PFC in executive function in humans (Bechara et al., 1998; Hornak et al., 2004), non-human primates (Funahashi et al., 1993; Rygula et al., 2010) and rodents (Kellendonk et al., 2006; Schoenbaum et al., 2002), the function of the MD in cognition is more controversial. Whereas a number of groups have reported an impairment in working memory and reversal learning tasks in MD lesioned rats (Bailey and Mair, 2005; Block et al., 2007; Chudasama et al., 2001; Floresco et al., 1999; Hunt and Aggleton, 1998), several other studies did not observe such effects (Beracochea et al., 1989; Hunt and Aggleton, 1991; Mitchell and Dalrymple-Alford, 2005; Neave et al., 1993).

The interpretation of lesion studies is difficult in the context of imaging studies. Indeed, imaging studies have merely reported a decrease in the activity of the MD, while lesion studies physically and irreversibly ablate the entire structure. Imaging studies further suggest that the MD cooperates with the PFC during cognitive processes, but the nature of this relationship cannot be addressed by lesion studies in which both structures do not remain intact. To address these questions and to circumvent these limitations, we therefore used a recently developed pharmacogenetic approach, the DREADD (Designer Receptor Exclusively Activated by a Designer Drug) system (Armbruster et al., 2007; Garner et al., 2012; Ray et al., 2011) to selectively and reversibly decrease neuronal activity in the MD of mice performing cognitive tasks. We found that a relatively mild decrease in the activity of MD neurons is sufficient to trigger selective impairments in two prefrontal dependent cognitive tasks: an operant-based reversal learning task and a delayed non-matching to sample (DNMS) working memory task. To investigate the nature and the role of MD-PFC communication in working memory we recorded simultaneously from both structures in mice performing the DNMS task. We found that synchronous activity between MD and medial PFC (mPFC) increased hand in hand with choice accuracy during the learning of the task and that reducing MD activity delayed both learning and the strengthening of synchrony. Interestingly, in trained animals, the strength of MD neurons phase-locking to medial prefrontal oscillations in the beta frequency range (13-30 Hz) increased specifically during the choice phase of the task associated with peak mnemonic demand, suggesting a role for MD-PFC beta synchrony in working memory. Strikingly, a primary decrease in the firing of MD neurons selectively disrupted this task-specific increase in MD-PFC beta-synchrony. In conclusion, our results demonstrate a causal relationship between decreased MD activity and deficits in executive function. They further suggest thalamo-frontal beta synchrony as a potential mechanism contributing to working memory.

RESULTS

Decrease of medio-dorsal thalamus neurons activity using DREADD system

A modified human muscarinic receptor, hM4D, was co-expressed along with humanized renilla green fluorescent protein (hrGFP) selectively in the MD using an adeno-associated virus expression system (AAV2-hM4D-IRES-hrGFP) (Figure 1A). The hM4D receptor is activated solely by a pharmacologically inert compound, clozapine-*N*-oxide (CNO), and not by endogenous acetylcholine or any other neurotransmitter. Upon CNO activation, hM4D hyperpolarizes neurons through a G-protein mediated activation of inward-rectifying potassium channels (Armbruster et al., 2007). Stereotactic injection of AAV2-hM4D-IRES-hrGFP virus into the MD induced co-expression of both GFP (green) and hM4D as assessed by anti-HA immunostaining (red) (Figure 1B). At higher magnification, we observed that the hM4D is localized in the plasma membrane as well as in neuronal processes (Figure 1B, D). Co-staining with anti-NeuN antibodies revealed that GFP expression was exclusively neuronal (Figure 1C top panel). Due to the absence of interneurons in rodents MD (Kuroda et al., 1998), all infected neurons should be relay projection neurons. Using AAV2.2, an average of 27 ±6% of the MD neurons expressed the GFP with a peak at 66 ±9.6% at the site of injection (Figure 1C bottom panel). The virus spread almost entirely among the anterio-posterior axis of the MD whereas it stayed constrained within the dorso-ventral and latero-medial axis of the MD (Figure 1C and S1A). Consistent with the known anatomy of the MD (Kuroda et al., 1998), infected neurons projected to layers I and III/V of prelimbic and orbito-frontal cortices (Figure 1D).

To determine whether activation of hM4D will hyperpolarize thalamic neurons as has been shown for hippocampal neurons (Armbruster et al., 2007), we performed whole-cell patch clamp recordings from thalamic slices. Fluorescently-identified neurons expressing hM4D were significantly hyperpolarized after CNO bath application, while the resting membrane potential of cells infected with a control virus expressing only hrGFP were not (Figure 2A). To determine whether activation of hM4D reduces the activity of MD neurons *in vivo*, we performed multiple single-unit recordings from the MD of freely moving mice injected with AAV2-hM4D-IRES-hrGFP (MD_{hM4D} mice). For this experiment, mice were exploring a familiar environment, specifically a T-maze to which they had been previously habituated. 63 single-units were recorded both after systemic injection of saline and 2 mg/kg CNO. The dose of CNO was chosen based on a previous study reporting high in vivo efficacy at doses between 1 and 5 mg/kg on locomotor activity and stereotypy in a transgenic mouse expressing the hM3Dq receptor within the forebrain (Alexander et al., 2009). CNO reduced the firing rate of a substantial portion of the MD units (Figure 2B-D). To quantify this effect, we first calculated the ratio of firing rates after saline and CNO for each unit; the distribution of ratios in the sample was significantly different than that expected by chance ($p<0.01$, Wilcoxon signed-rank test) (Figure 2C). We next compared firing rates after saline and CNO injections for each neuron independently. CNO decreased firing rate significantly ($p<0.05$ by paired t-test) in 30 neurons (48%). In an additional 11 units (17%), CNO increased the firing rate. Using a more stringent Bonferroni correction ($p<0.0008$) 16 (25%) and 6 (9.5%) units were inhibited or activated by CNO, respectively. For both analyses neurons with decreased firing rate were overrepresented as a consequence of CNO treatment (Binomial test: $p<0.01$, $p<0.05$ for Bonferonni-corrected values). Importantly, CNO treatment did not completely silence MD neurons; the neurons with decreased firing rate showed an average decrease of 38.7+-5.3%. This decrease in firing rate was not related to changes in locomotor activity or to differences in the isolation of single units (Figure S2A-C). The CNO-mediated decrease in firing rate was not observed in wild type mice that do not express hM4D, demonstrating its dependence on hM4D (Figure 2C inset). While hyperpolarization of thalamic cells can induce a shift in the firing pattern from a tonic to a bursting mode due to the activation of T-type Ca^{2+} channels (Jahnsen and Llinas, 1984), we

did not observe a significant change in the fraction of burst firing *in vivo* after CNO injection (Figure S2D).

Decreasing MD activity leads to deficits in tasks addressing behavioral flexibility and working memory

Due to the strong projections of the MD to the orbital-frontal cortex (Figure 1E) we first tested whether decreasing MD activity affects reversal learning, a cognitive process of executive function that is sensitive to orbito-frontal (OFC) lesions (Schoenbaum et al., 2002). To address reversal learning, we developed an operant-based reversal learning task for the mouse in which lever presses are rewarded in the presence of one visual cue (S+), but not in the presence of another visual cue (S-) (discrimination phase). After mice reached criterion the contingencies were reversed (reversal phase) (Figure 3A). The acquisition of the discrimination phase was not affected by decreasing MD activity (repeated ANOVA $p=0.17$) though CNO-treated MD_{hM4D} mice showed a tendency for a delay in learning during the first three days of acquisition (Figure 3B). In contrast, reversal learning was clearly impaired in CNO-treated MD_{hM4D} mice when compared to the three control groups (repeated ANOVA followed by bonferroni correction for group comparisons $*p<0.05$, $**p<0.01$) (Figure 3C). As has been observed for OFC lesions, these deficits were likely due to perseverative behavior, as mice with reduced MD activity made significantly more S- responses (previously rewarded during the discrimination phase) than the control groups over the seven sessions of the reversal phase (repeated ANOVA followed by bonferroni correction for group comparisons $*p<0.05$, $***p<0.001$) (Figure 3D). This perseverative behavior was evident even within the first trials of the first reversal session, in which control mice were able to repress their number of S- responses while CNO-treated MD_{hM4D} mice were not (Figure S3A and B).

To address working memory, we performed a delayed non-matched to sample (DNMS) T-maze task commonly used in rodents (Figure 4A). Deficits in both acquisition and performance of this task have been observed after lesioning or silencing the mPFC in rats and mice (Dias and Aggleton, 2000; Kellendonk et al., 2006; Yoon et al., 2008). Similarly, decreasing MD activity with CNO led to a deficit in the acquisition of the task, as CNO-treated MD_{hM4D} mice showed took longer to reach learning criterion than controls (ANOVA followed by Newman-Keuls correction for group comparisons $*p<0.05$) (Figure 4B). To determine whether decreasing MD activity also affects working memory performance, a second cohort of hM4D- and GFP-expressing mice was trained without CNO until they reached criterion (Figure S4A). Working memory performance was then tested after CNO or saline treatment at delays ranging from 6 to 120 s. In this cohort the number of animals was too low for a statistical comparison of all four groups. Since the three control groups did not differ in their performance (Figure S4B), they were combined for their comparison with CNO-treated MD_{hM4D} mice. CNO-treated MD_{hM4D} mice performed as well as the controls on the shorter delays (6 and 30 s) but showed significantly poorer performance on longer delays (repeated ANOVA group effect $**p<0.01$) (Figure 4C). The observed deficits were not due to a general attention deficit or deficits in learning the spatial contingencies of the task, as mice with decreased MD activity showed performance comparable to that of control mice in a T-maze based spatial reference memory task (Figure 4D). Moreover, we did not observe any general alterations of locomotor activity or anxiety-like behavior as assessed in open field and elevated plus maze tests that may interfere with performance in the reversal learning or in the DNMS T-maze task (Figure S4C and D).

Working memory-induced modulation of thalamo-prefrontal beta synchrony is disrupted by low MD activity

Based on imaging studies reporting deficits in functional connectivity between different areas of the brain in patients, the disconnection theory (Pettersson-Yeo et al., 2011) posits schizophrenia as a subtle but pernicious syndrome of decreased long-range connectivity. In agreement with this theory, alterations in functional connectivity between MD and PFC have been observed in patients engaged in executive function tasks, including working memory (Minzenberg et al., 2009; Mitelman et al., 2005). To determine whether spatial working memory in mice involved MD-PFC synchrony, we recorded neural activity simultaneously in the MD and mPFC of mice performing the T-Maze DNMS task. If MD-PFC synchrony is involved in working memory, it should specifically be modulated during the choice phase of the DNMS T-Maze task, when the mnemonic requirement is high. For example, recent studies have shown that theta-frequency synchrony between the dorsal hippocampus (dHPC) and mPFC is modulated by the DNMS task (Jones and Wilson, 2005; Sigurdsson et al., 2010). These studies found that phase-locking of PFC units to the theta-frequency component of the hippocampal local field potential (LFP) was enhanced during the choice phase of the DNMS task (which requires working memory) compared to the sample phase (which does not).

We therefore examined MD unit phase-locking to mPFC LFPs across multiple frequency ranges in trained animals performing the DNMS T-maze task. In saline treated mice, the phase-locking of MD units to beta-frequency (13-30 Hz), but not theta (4-12 Hz) or gamma-frequency (40-60 Hz) PFC oscillations, was strengthened in the choice phase (two tailed paired t-test, **$p<0.01$) (Figure 5A) suggesting that MD-PFC synchrony in the beta range is selectively modulated by working memory. Looking at individual units, about half of units (17/40; 42.5%) noticeably increased their phase locking to mPFC beta-oscillations during choice phase while phase-locking did not change or decreased in 18/40 (47.5%) and 4/40 (10%) units, respectively (Figure S5A). Strikingly, the increase in MD-PFC beta synchrony was selectively disrupted in CNO-treated MD_{hM4D} mice (repeated ANOVA, task phase x treatment interaction #$p<0.05$) (Figure 5A). This was observed as well in mice that never received CNO injection prior the recording ruling out that these effects could be due to chronic effects of the drug (Figure S5E). Phase-locking to other frequency ranges was unaffected. Examining individual cells, we observed a significant reduction (Odd ratio=0.09, $p<0.001$) of the percentage of neurons increasing their phase locking (2/33; 6.1%) and a significant increase (Odd ratio=5.5, $p<0.01$) of the percentage of cells showing no changes (27/33; 81.8%) in CNO-treated mice compared to controls (Figure S5A). The effects of decreasing MD activity on the sample/choice difference in phase-locking was also confirmed using the pairwise phase consistency measure that controls for spike history effects such as bursting (Figure S5F) (Vinck et al., 2012).

To rule out the possibility that CNO-treatment affected the quality of unit isolation, we confirmed that this disruption in MD-PFC beta synchronization was not due to differences in unit quality (Figure S5B and C). To examine the specificity of disrupted communication between the MD and mPFC we also measured synchrony between the MD and the dHPC, a structure that is also important for spatial working memory. While no task-related modulation of phase-locking strength was observed in the beta and gamma range, a decrease of phase locking between MD single-unit activity and dHPC theta-oscillations occurred during the choice phase of the DNMS task (Figure 5B, two tailed paired t-test, ***$p<0.001$). However, this decrease was not altered by CNO treatment (Figure 5B). Power spectra in the MD and mPFC were unchanged by CNO, suggesting that the effects of reducing MD activity were specific to the connectivity between the two regions rather than alterations in the strength of oscillations in either region (Figure S5D). We also examined the effects of CNO task-related firing in the recorded MD units, examining whether firing rates in the start

arm of the T-maze were modulated across sample vs. choice, right vs. left, or error vs. correct trials. In saline treated mice, 40% (21/51) of our recorded units were firing in a task-related manner. We saw a non-significant trend towards a reduction in the percentage of task-related MD cells in CNO-treated mice as 31% (17/54) exhibited task-related activity.

Together, these results suggest that decreasing MD activity may impair working memory by disrupting MD-PFC beta synchrony during the choice phase of the task. In line with this interpretation, we found an increase of the proportion of MD cells significantly phase locked to mPFC beta oscillations when trained control mice were performing the task (61/69 cells, 88%) compared to mice that were simply exploring the maze (15/59 cells, 25%) (Odds ratio=22.37, $p<0.001$). Lag analysis revealed a predominant MD to mPFC directionality in the beta-frequency range. Phase locking of each MD unit was calculated repeatedly after systematically shifting the MD action potentials forward and backward in time relative to the mPFC LFP (Siapas et al., 2005). MD units tended to phase lock strongest to the mPFC beta-frequency oscillation of the future (mean lag, +20 ± 1.4 ms, wilcoxon signed rank test $p<0.05$, $n=76$) (Figure 5C). This finding is consistent with the possibility that information tends to flow from the MD to the mPFC during the DNMS task.

Beta-frequency synchrony parallels behavior during working memory task acquisition

The parallel effects of MD inhibition on phase-locking and behavior after successful task acquisition suggest a role for the MD and MD-PFC connectivity in working memory performance. Yet CNO-treated MD_{hM4D} mice also had a deficit in task acquisition (Figure 4B). To determine whether altered MD-PFC functional connectivity could account for the deficits observed in task acquisition observed in CNO-treated MD_{hM4D} mice, we examined MD-PFC synchrony in an additional cohort of MD_{hM4D} mice treated with daily injections of CNO or saline during acquisition of the DNMS T-maze task. Because the training period is too brief to permit recording of a sufficient sample of MD units, coherence between MD and PFC LFPs was used to measure synchrony. As with the first cohort, CNO-injected MD_{hM4D} mice took significantly longer to acquire the task than saline-injected MD_{hM4D} mice (Figure S6A and B). Consistent with a role for MD-PFC connectivity in task learning, LFP coherence between these two structures increased with task acquisition in both CNO- and saline injected MD_{hM4D} mice (Figure 6A and S6C). Strikingly, coherence in beta-frequency range increased hand in hand with performance (Figure 6B). In control mice, increases in coherence and choice accuracy occurred simultaneously at the end of 2nd session (trials 15-20). In contrast, both coherence and choice accuracy started to increase later in CNO-treated MD_{hM4D} mice (session 5, trials 41-45) (repeated ANOVA followed by Fischer correction, difference vs trials 1-5: °$p<0.1$, *$p<0.05$, **$p<0.01$, ***$p<0.001$). In addition, we did an analysis of correlation between coherence and performance for each session and each individual animal and found that coherence correlated significantly with behavioral performance for both saline- and CNO-treated MD_{hM4D} mice. Finally, the parallel increase of coherence and performance was also seen in the theta-frequency range (Figure S6D-E). In contrast, while gamma-frequency coherence also increased between early and late training phases in both saline and CNO-treated MD_{hM4D} mice, these increases did not correlate with increases in choice accuracy (Figure S6B-E). These data, together with the phase-locking findings, demonstrate that inhibition of MD disrupts both MD-PFC functional connectivity and working memory behavior in parallel, during task acquisition as well as task performance.

DISCUSSION

Imaging studies have repeatedly reported deficits in MD and PFC activation in schizophrenia patients performing cognitive tasks. However, whether a decrease in MD activity can cause cognitive deficits is unclear. Moreover, the potential role for MD-PFC

dysconnectivity in the generation of cognitive symptoms still remains unexplored. Here, by inducing a subtle decrease in the firing of MD neurons, we triggered selective deficits in two prefrontal-dependent tasks that address reversal learning and working memory, cognitive processes impaired in patients with schizophrenia. We further found that beta range synchrony between the MD and the mPFC is modulated by working memory, and that this modulation is disrupted by the decrease in MD activity. Finally, during DNMS task acquisition, the magnitude of MD-PFC coherence increased in tight correlation with choice accuracy and both increases were delayed by inhibition of MD activity. Together these data demonstrate that decreased MD activity disrupts functional communication within the MD-PFC circuit and causes deficits in prefrontal-dependent cognition. Our findings are consistent with a role for MD-PFC synchrony in working memory tasks, and further support the possibility that thalamic deficits can causally contribute to cognitive dysfunction.

The role of MD activity in behavioral flexibility and working memory

Decreasing MD activity specifically impaired reversal learning while sparing the initial discrimination learning. One brain area that is implicated in reversal learning and receives direct projection from the MD is the OFC. It is therefore possible that disrupted communication between these two structures may underlie the observed deficit in reversal learning. In fact, both humans and non-human primates with damage to OFC are unimpaired on discrimination tasks but show deficits in reversing stimulus-reward association within a particular perceptual dimension (Berlin et al., 2004; Dias et al., 1997). As in primates, OFC lesions in rats have been shown to impair reversal learning (Boulougouris et al., 2007; Schoenbaum et al., 2002). Moreover OFC lesions across species have been repeatedly associated with increase perseveration during reversal learning (Boulougouris et al., 2007; Dias et al., 1996; Rolls et al., 1994). We also found that decreasing MD activity increased perseverative errors during reversal phase. Indeed, CNO-treated MD_{hM4D} mice responded more during the presentation of the previously rewarded cue than the controls. This phenomenon was already observed within the first session, during which controls but not CNO-treated MD_{hM4D} mice are able to repress their number of S- responses (Figure S3). It is unlikely that this increase of S- responses during the reversal was due to general hyperactivity because CNO-treated MD_{hM4D} mice did not show hyperactivity in other behavioral tasks, such as open field testing (Figure S4). Moreover, decreasing MD activity did not increase the number of lever presses during the discrimination phase (data not shown). As OFC lesions have been associated with impulsive behavior in humans (Berlin et al., 2004), it is possible that CNO-treated MD_{hM4D} mice may simply be unable to repress S- responses due to increased impulsivity. This explanation is however unlikely because CNO-treated MD_{hM4D} mice did not show a deficit in repressing S- responses during the discrimination phase.

We further showed that a decrease in MD activity induced a deficit in the acquisition in a DNMS working memory task. This impairment is not due to a deficit in general attention or deficits in learning the spatial contingencies of the task because CNO-treated MD_{hM4D} mice had no problems in learning a spatial version of the T-maze task. Decreasing MD activity not only impaired the acquisition but also the performance of the DNMS task in trained animals, sparing performance at short (6 to 30 s) delays but impairing performance at long delays (60 to 120 s). One brain area that is implicated in working memory and receives direct projection from the MD is the mPFC. Deficits in both acquisition and performance of the DNMS T-maze task have been observed after lesioning or silencing the mPFC in rats and mice (Dias and Aggleton, 2000; Kellendonk et al., 2006; Yoon et al., 2008). We therefore hypothesize that disrupted communication between the MD and mPFC may underlie the observed deficit in the working memory task. Our electrophysiological findings discussed below are in line with this interpretation.

MD-PFC functional connectivity during working memory

Here we report increases in synchrony between the MD and mPFC during a spatial working memory task in control mice. During task acquisition, synchronized activity between these two structures in the theta- and beta-frequency ranges increased hand in hand with improvements in task performance. After successful acquisition, beta-frequency synchrony was specifically enhanced in the working memory-requiring choice phase of the task, during which mice need to keep information online to make the correct choice and obtain the reward. Finally, lag analysis demonstrated that the MD leads the mPFC. These results are consistent with the hypothesis that information flows from the MD to the mPFC in support of working memory, similar to previous findings suggesting that hippocampal-prefrontal interactions are also involved (Jones and Wilson, 2005; Sigurdsson et al., 2010). The precise nature of the information contributed by MD inputs to the m PFC is unclear. Studies of MD single unit activity during visual working memory in non-human primates have suggested the possibility that MD units encode motor planning information (Watanabe and Funahashi, 2012). Considering the known inputs to the MD from the striatum and extrapolating from these findings, it may be that the MD transmits motor information to the PFC about the choice to be made during spatial working memory.

Our findings point to synchrony between the MD and mPFC in the beta-frequency (13 to 30 Hz) range as of particular relevance to the DNMS task. While the oscillations in the theta and gamma bands have been classically linked to working memory, the functional role of beta-band oscillations is less understood. However, recent studies performed in human and non-human primates point to a role for beta-band oscillations in cognitive processes. Specifically, elevations of beta-band activity in visual and prefrontal cortical areas have been observed during the delay phase of working memory tasks (Deiber et al., 2007; Siegel et al., 2009; Tallon-Baudry et al., 2001; Tallon-Baudry et al., 2004). Interestingly, beta-band activity has also been linked to motor activity. Indeed, numerous studies provided the evidence that beta activity is decreased during voluntary movements and increased during holding periods following movement in a variety of structures belonging to the motor system (for a review see (Engel and Fries, 2010)). Rather than reflecting a lack of movement, a recent hypothesis proposed that beta rhythm would be related to the active maintenance of the current sensorimotor set. According to this hypothesis, the role of beta oscillations in cognition would be of similar nature and may be enhanced if the status quo is given priority over distractive new signal, whereas gamma band activity may predominate if changes in stimulus are expected (Engel and Fries, 2010). Therefore, beta oscillations may relate to top-down processing and the increase of MD-PFC beta coherence observed during the choice phase of the DNMS task may reflect the maintenance of the information previously acquired during the sample phase of the task.

MD-PFC dysfunction in schizophrenia

The current findings are of potential relevance to the understanding of cognitive deficits in schizophrenia. Imaging studies reported both deficits in MD and PFC (Andrews et al., 2006; Minzenberg et al., 2009; Weinberger and Berman, 1996) in patients with schizophrenia during cognitive tests. Moreover recent studies have found an altered correlation in the activity of MD and PFC, suggesting that impaired functional connectivity between these structures might underlie the cognitive difficulties (Minzenberg et al., 2009; Mitelman et al., 2005). Structural abnormalities in this circuit have also been reported (Byne et al., 2009; Marenco et al., 2012). However, one limitation of brain imaging is the low temporal resolution that does not allow studying the complex spatial-temporal orchestration of brain activity that is thought to underlie cognition. EEG methods offer a better temporal resolution and some studies observed that synchronous activity of beta and gamma oscillations are decreased in the cortex of patients with schizophrenia (for a review see (Uhlhaas and Singer,

2010)). Our results indicate that the engagement of beta synchrony in working memory is not restricted only to cortical areas but could also extend to thalamo-cortical circuits, and more specifically, that beta-frequency oscillations may underlie thalamo-cortical communication during working memory performance.

Our results further suggest that disruption of MD-PFC beta synchrony could participate in the generation of cognitive deficits in schizophrenia. However, whether this disruption is of primary origin in schizophrenia is hard to determine due to the circular nature of the brain. Post mortem and structural brain imaging studies show morphological abnormalities in the MD that suggest a primary deficit of the MD, at least in a subpopulation of patients (Byne et al., 2009). However, the MD is also part of the well-described cortico-striatal loops in which the striatum projects back to the cortex via the thalamus (Haber and Calzavara, 2009). A primary role of the striatum for the pathogenesis of schizophrenia has been proposed (Simpson et al., 2010). In this context, we previously showed that overexpression of striatal dopamine D2 receptors, as a model for increased D2 receptor function observed in patients, causes PFC-dependent cognitive deficits. These deficits included impairments in the here presented DNMS T-maze working memory task (Kellendonk et al., 2006). One possibility is therefore that altered striatal function could impact on the prefrontal cortex via altering MD activity. Measuring MD-PFC synchrony in striatal D2 overexpressing mice would be a useful test of this hypothesis.

The DREADD system as a tool to decrease MD activity

In this study, we chose a pharmacogenetic approach to reversibly reduce MD activity. The DREADD system relies on a mutated human muscarinic G-protein coupled receptor that does not respond to the endogenous ligand acetylcholine. The activation of these receptors can be achieved by intraperitoneal injection of a biologically inert synthetic compound, CNO. There has been concern regarding the potential retro-reduction of CNO to clozapine, a well-known atypical antipsychotic drug (Loffler et al., 2012). However, for several reasons, our results cannot be explained by this back metabolism. First, while CNO retro-reduction to clozapine has been observed in humans and guinea pigs (Jann et al., 1994), back metabolism could not be detected in rats and mice (Guettier et al., 2009; Jann et al., 1994). Second, CNO-treated GFP-expressing control mice did not show any alteration in any of the tested behaviors compared to saline groups. This includes behavior that have been shown to be insensitive to clozapine such as locomotor activity (McOmish et al., 2012). Finally, clozapine has been reported to alter MD firing (Lavin and Grace, 1998). While we found a decrease in MD neuronal firing rate in MD_{hM4D} mice injected with CNO (Figure 2B-D) we did not see any firing rate changes in mice that do not express the hM4D receptor (Figure 2C inset).

CONCLUSION

A major limitation of clinical studies is that they cannot draw causal relations between observed anatomical/functional deficits and specific symptoms. Using pharmacogenetic tools in combination with *in vivo* recordings from awake behaving animals we found that even a subtle decrease in MD activity can lead to altered MD-PFC functional connectivity and prefrontal-dependent cognitive deficits. Based on these findings we propose that abnormalities found in the MD of patients with schizophrenia could participate to the pathogenesis of cognitive deficits.

EXPERIMENTAL PROCEDURES

Animals

All protocols used in the present study were approved by the Institutional Animal Care and Use Committee (IACUC) at Columbia University. Mice were C57/Bl6 males purchased from Jackson Laboratory and housed under a 12-h, light-dark cycle in a temperature-controlled environment with food and water available *ad libitum*. For the behavioral experiments (reversal learning and T-maze tasks) mice were food restricted and maintained at 85% of their initial weight. For this, they were limited to 1 h 30 daily access to food in the home cage. After testing, mice were sacrificed and the expression as well as the location of GFP expression was verified to ensure that we correctly targeted the MD (Figure S5). Mice for which GFP was not visible or in an incorrect location were removed from the final analysis.

Drugs

Clozapine-N-Oxide (CNO) (sigma) was dissolved in PBS to a final concentration of 0.2 mg/ml. PBS or CNO (2 mg/kg) was administered intra-peritoneal to the mice 30 min before behavioral testing or *in vivo* recording (based on personal observations and Alexander et al. 2009). For thalamic slice physiology CNO was diluted into 1 μM with artificial cerebrospinal fluid. Fresh CNO solution was prepared on the day of usage.

Generation of AAV2-hM4D and virus injection

The AAV2-hM4D-IRES-hrGFP (called later AAV2-hM4D) virus was generated by inserting the hM4D sequence into the multiple cloning site of the pAAV-IRES-hrGFP vector (Agilent Technologies). The AAV2-hM4D-IRES-hrGFP and control (AAV2-hrGFP) viruses were produced by Vector Biolabs (Eagleville, PA). Mice were injected bilaterally with 0.5 μl of AAV2-hM4D (1.04×10^{13} particles/ml) or AAV2-hrGFP (1×10^{12} particles/ml). Viruses were pressure injected using a glass pipette (10-15 μm) into the MD (coordinates: A/P, -1.3 mm; M/L, ±0.35 mm; D/V, -3.2 mm). After each injection, the pipette remained *in situ* for 10 min to minimize leaking. 6 weeks-old mice were injected and then tested 4 weeks later for both behavioral and *in vivo* electrophysiology studies. For thalamic slice recordings, 3 weeks-old mice were injected and sacrificed 3 weeks later.

Histology and immunostaining

Histology and immunostaining was performed using classical methods (see supplemental for more details). HA rabbit-polyclonal (Invitrogen # 71-5500) antibody was diluted 1/1000 in PBS and incubated overnight at 4dC. Anti NeuN (Millipore, MAB377) HC was performed at a dilution of 1/100. The anti-rabbit Cy3 secondary antibody (Jackson laboratories) was diluted 1/1000.

Behavior

Reversal learning task

Discrimination phase: This phase was done under a VI 20 s schedule. During the discrimination task, lever presses were reinforced depending on which of two visual stimuli (a flashing and a steady house light) were present. Lever presses in the presence of one of the stimuli (S+) were rewarded according to the VI 20 s schedule. Lever presses in the presence of the other stimulus (S-) did not lead to any reward. One session was composed by 20 S+ and 20 S- trials. S+ and S- trials were selected randomly and were separated by a variable ITI during which the house light was turned off. The duration of S+ trials was 1 min. Thus, the average number of rewards earned during S+ trials was 60. S- trials were also 1 min in duration. However a 20 s penalty was included such that mice were required to

withhold lever presses for 20 s in order for the next trial to commence. l. Mice performed one session per day, and the discrimination phase ended after 7 sessions were completed.

Reversal phase: During this phase, all experimental events occurred in the same manner as the discrimination phase, except that the reward contingencies were reversed so that the S+ became S- and vice versa. One session was composed by 20 S+ trials and 20 S-. Again, mice performed one session per day, and the reversal phase ended after 7 sessions were completed.

Non-Matching to sample T-maze task—We used the methods described previously (Sigurdsson et al., 2010). Briefly, mice were tested on 10 trials per day, each trial consisting of two runs, a forced run and a choice run. To obtain a reward, animals were required to enter the goal arm not visited during the forced phase. Animals were given daily training sessions of 10 trials until they reached criterion performance, defined as performance of a minimum of seven trials correct per day for three consecutive days. After the mice reached criterion, there performance was tested on different delays of 6 s, 30 s, 60 s, 90 s, 120 s and 180 s with 10 trials per delay.

Spatial T-maze task—The spatial version of the T-maze used the same maze apparatus and habituation procedure than the non-matching to sample task. Only the rule to acquire the task differed. For all trials each mouse was assigned one arm, left or right, as the baited target arm. Mice use an allocentric or spatial strategy to solve this task. Mice were trained ten trials per day and criterions were fixed at seven correct choices out of ten during three consecutive days.

In Vivo recordings

Microdrive construction and Surgery—Animals were implanted with multiwire microdrives using methods described previously (Adhikari et al., 2010). For more details, see supplemental methods.

Behavior and neurophysiological data acquisition—Mice used for “task independent” MD single unit activity (Figure 2B-D) were recorded during free exploration of the T-maze. Mice were injected i.p. with saline solution and recorded 30 minutes after the injection during 15 minutes. After this, without moving the stereotrodes, mice were injected i.p. with CNO and recorded 30 minutes after the injection during 15 minutes. Mice used for “working memory task dependent” recordings were performing the previously described T-maze DNMS task during data acquisition. We restricted our analysis to neural activity in the center arm of the maze during sample and choice phases. This had the advantage of minimizing behavioral variability, as both trajectories and speeds of center-arm runs were comparable in saline- and CNO-treated and MD_{hM4D} mice. Recordings were obtained via a unitary gain head-stage preamplifier (HS-32; Neuralynx) attached to a fine wire cable. Field potential signals from MD, mPFC and dHPC sites were recorded against a screw implanted in the anterior portion of the skull. LFPs were amplified, bandpass filtered (1–1,000 Hz) and acquired at 1893 Hz. Spikes exceeding 40 μV were bandpass-filtered (600–6,000 Hz) and recorded at 32 kHz. Both LFP and spike data were acquired with Lynx 8 programmable amplifiers on a personal computer running Cheetah data acquisition software (Neuralynx). The animal's position was obtained by overhead video tracking (30 Hz) of two light-emitting diodes affixed to the head stage.

Firing rate and burst analysis—Data was imported into Matlab for analysis using custom-written software. Instantaneous firing rate for the example cell in Figure 2B was smoothed using Matlab smooth with a 60s moving average. To test the significance of firing

rate changes, we used both a population analysis and an individual cell analysis. For the population analysis we used a sign rank test to determine whether the distribution of firing rate rations (CNO:SAL) were significantly different from a distribution with a median of 1. For the individual cell analysis each 15 min recording session under either saline or CNO conditions were separated into 30s bins and firing rate was calculated. A one-factor ANOVA was performed on each cell to determine whether the mean firing rate after CNO was significantly different from that after SAL, with and without Bonferroni correction as described in the text. The predominance of decreases vs. increases in firing rate using this method was then also tested using a Binomial test. For burst analysis, a burst was defined by the following criteria: maximum interval to start burst (i.e., the first interspike interval within a burst) must be =4 ms; maximum interval to end burst, 10 ms; minimum interval between bursts, 100 ms; minimum duration of burst, 4 ms; and minimum number of spikes within a burst, two.

Phase locking analysis—Phase locking of MD units to mPFC LFPs was accomplished by fist filtering the field potentials in either the theta (4-12 Hz) beta (13-30Hz) or gamma (40-60Hz) range using a zero phase delay filter and computing phase using a Hilbert transform. Each unit spike was assigned a phase based on its simultaneous field potential sample. The magnitude of phase locking was quantified mean resultant length (MRL) of the sum of the unit vectors representing the phases at which each spike occurred, divided by the number of spikes. The MRL is sensitive to the number of spikes used in the analysis. Therefore, to compare phase locking strength by condition we computed the MRL for multiple (1000) subsamples of 50 spikes per condition and averaged across subsamples for each condition, and for each unit. Units that fired fewer than 50 spikes in each condition were not analyzed. The statistical significance of phase-locking was assessed using the Rayleigh test for circular uniformity.

Directionality Analysis—Data was pooled for task independent and task dependent behavior sessions. Cells with fewer than 600 spikes during the entire recording session were not analyzed. To determine the temporal relationship between unit activity and beta oscillations in the mFPC, phase locking was calculated for 50 different temporal offsets from the mPFC LFP for each unit recording. Only units with significant Bonferroni-corrected phase locking in at least one of the 50 shifts are shown in Figure 5C.

Field Potential Analysis—For coherence and behavior across learning, recordings were binned into early (first 5 trials), middle (trials 25-30) and late (last 5 trials on the day the animal achieved criterion performance) trials. Coherence of the field potentials was computed using the multitaper method (MATLAB routines provided by K. Harris). Field potential samples for the trials in each bin were concatenated and then divided into 1000 ms segments (800 ms overlap). The Fourier transform of each segment was computed after being multiplied by two orthogonal data tapers. Coherence was computed by averaging the cross-spectral densities of two field potential signals across data windows and tapers and normalizing to the power spectral densities of each signal. Beta coherence was computed as the mean coherence in the 13-30 Hz range.

Supplementary Material

Refer to Web version on PubMed Central for supplementary material.

Acknowledgments

We would like to thank Neil Harrison for advising on *in vitro* slice physiology and Mariya Shegda for excellent technical help. CNO was obtained from the NIH as part of the Rapid Access to Investigative Drug Program funded

by the NINDS. This work was supported by grants from “Anonymous Foundation”, and NARSAD to C.K. from the International Mental Health Research Organization, the Hope for Depression Research Foundation, and the NIH (R21 MH093887 and R01 MH081968) to J.A.G, U19MH82441 to B.L.R. and a Fondation Fyssen Fellowship to S.P. A.A. is a Leon Levy Foundation Resident Fellow and is supported by R25 MH086466.

S.P. designed and performed the experiments, conducted the data analysis and wrote the paper. P.K.O. performed the in vivo recordings experiment and conducted the analysis. S.B. and R.W helped with behavior experiments. A.A. assisted in the analysis of the in vivo recordings. B.L.R. provided plasmids. P.B. supervised the performance of behavior experiments. J.A.G. and C.K. designed the experiments, supervised the performance of the experiments and data analysis, and wrote the paper.

REFERENCES

Adhikari A, Topiwala MA, Gordon JA. Synchronized activity between the ventral hippocampus and the medial prefrontal cortex during anxiety. Neuron. 2010; 65:257–269. [PubMed: 20152131]

Alexander GM, Rogan SC, Abbas AI, Armbruster BN, Pei Y, Allen JA, Nonneman RJ, Hartmann J, Moy SS, Nicolelis MA, et al. Remote control of neuronal activity in transgenic mice expressing evolved G protein-coupled receptors. Neuron. 2009; 63:27–39. [PubMed: 19607790]

Andrews J, Wang L, Csernansky JG, Gado MH, Barch DM. Abnormalities of thalamic activation and cognition in schizophrenia. The American journal of psychiatry. 2006; 163:463–469. [PubMed: 16513868]

Armbruster BN, Li X, Pausch MH, Herlitze S, Roth BL. Evolving the lock to fit the key to create a family of G protein-coupled receptors potently activated by an inert ligand. Proceedings of the National Academy of Sciences of the United States of America. 2007; 104:5163–5168. [PubMed: 17360345]

Bailey KR, Mair RG. Lesions of specific and nonspecific thalamic nuclei affect prefrontal cortex-dependent aspects of spatial working memory. Behavioral neuroscience. 2005; 119:410–419. [PubMed: 15839787]

Bechara A, Damasio H, Tranel D, Anderson SW. Dissociation Of working memory from decision making within the human prefrontal cortex. J Neurosci. 1998; 18:428–437. [PubMed: 9412519]

Beracochea DJ, Jaffard R, Jarrard LE. Effects of anterior or dorsomedial thalamic ibotenic lesions on learning and memory in rats. Behavioral and neural biology. 1989; 51:364–376. [PubMed: 2730499]

Berlin HA, Rolls ET, Kischka U. Impulsivity, time perception, emotion and reinforcement sensitivity in patients with orbitofrontal cortex lesions. Brain. 2004; 127:1108–1126. [PubMed: 14985269]

Block AE, Dhanji H, Thompson-Tardif SF, Floresco SB. Thalamic-prefrontal cortical-ventral striatal circuitry mediates dissociable components of strategy set shifting. Cereb Cortex. 2007; 17:1625–1636. [PubMed: 16963518]

Boulougouris V, Dalley JW, Robbins TW. Effects of orbitofrontal, infralimbic and prelimbic cortical lesions on serial spatial reversal learning in the rat. Behavioural brain research. 2007; 179:219–228. [PubMed: 17337305]

Byne W, Hazlett EA, Buchsbaum MS, Kemether E. The thalamus and schizophrenia: current status of research. Acta neuropathologica. 2009; 117:347–368. [PubMed: 18604544]

Chudasama Y, Bussey TJ, Muir JL. Effects of selective thalamic and prelimbic cortex lesions on two types of visual discrimination and reversal learning. The European journal of neuroscience. 2001; 14:1009–1020. [PubMed: 11595039]

Deiber MP, Missonnier P, Bertrand O, Gold G, Fazio-Costa L, Ibanez V, Giannakopoulos P. Distinction between perceptual and attentional processing in working memory tasks: a study of phase-locked and induced oscillatory brain dynamics. Journal of cognitive neuroscience. 2007; 19:158–172. [PubMed: 17214572]

Dias R, Aggleton JP. Effects of selective excitotoxic prefrontal lesions on acquisition of nonmatching- and matching-to-place in the T-maze in the rat: differential involvement of the prelimbic-infralimbic and anterior cingulate cortices in providing behavioural flexibility. The European journal of neuroscience. 2000; 12:4457–4466. [PubMed: 11122356]

Dias R, Robbins TW, Roberts AC. Dissociation in prefrontal cortex of affective and attentional shifts. Nature. 1996; 380:69–72. [PubMed: 8598908]

Dias R, Robbins TW, Roberts AC. Dissociable forms of inhibitory control within prefrontal cortex with an analog of the Wisconsin Card Sort Test: restriction to novel situations and independence from “on-line” processing. J Neurosci. 1997; 17:9285–9297. [PubMed: 9364074]

Engel AK, Fries P. Beta-band oscillations--signalling the status quo? Current opinion in neurobiology. 2010; 20:156–165. [PubMed: 20359884]

Floresco SB, Braaksma DN, Phillips AG. Thalamic-cortical-striatal circuitry subserves working memory during delayed responding on a radial arm maze. J Neurosci. 1999; 19:11061–11071. [PubMed: 10594086]

Forbes NF, Carrick LA, McIntosh AM, Lawrie SM. Working memory in schizophrenia: a meta-analysis. Psychological medicine. 2009; 39:889–905. [PubMed: 18945379]

Funahashi S, Bruce CJ, Goldman-Rakic PS. Dorsolateral prefrontal lesions and oculomotor delayed-response performance: evidence for mnemonic “scotomas”. J Neurosci. 1993; 13:1479–1497. [PubMed: 8463830]

Garner AR, Rowland DC, Hwang SY, Baumgaertel K, Roth BL, Kentros C, Mayford M. Generation of a synthetic memory trace. Science. 2012; 335:1513–1516. [PubMed: 22442487]

Green MF. What are the functional consequences of neurocognitive deficits in schizophrenia? The American journal of psychiatry. 1996; 153:321–330. [PubMed: 8610818]

Guettier JM, Gautam D, Scarselli M, Ruiz de Azua I, Li JH, Rosemond E, Ma X, Gonzalez FJ, Armbruster BN, Lu H, et al. A chemical-genetic approach to study G protein regulation of beta cell function in vivo. Proceedings of the National Academy of Sciences of the United States of America. 2009; 106:19197–19202. [PubMed: 19858481]

Haber SN, Calzavara R. The cortico-basal ganglia integrative network: the role of the thalamus. Brain research bulletin. 2009; 78:69–74. [PubMed: 18950692]

Haenschel C, Bittner RA, Waltz J, Haertling F, Wibral M, Singer W, Linden DE, Rodriguez E. Cortical oscillatory activity is critical for working memory as revealed by deficits in early-onset schizophrenia. J Neurosci. 2009; 29:9481–9489. [PubMed: 19641111]

Hornak J, O'Doherty J, Bramham J, Rolls ET, Morris RG, Bullock PR, Polkey CE. Reward-related reversal learning after surgical excisions in orbito-frontal or dorsolateral prefrontal cortex in humans. Journal of cognitive neuroscience. 2004; 16:463–478. [PubMed: 15072681]

Hunt PR, Aggleton JP. Medial dorsal thalamic lesions and working memory in the rat. Behavioral and neural biology. 1991; 55:227–246. [PubMed: 2059189]

Hunt PR, Aggleton JP. Neurotoxic lesions of the dorsomedial thalamus impair the acquisition but not the performance of delayed matching to place by rats: a deficit in shifting response rules. J Neurosci. 1998; 18:10045–10052. [PubMed: 9822759]

Jahnsen H, Llinas R. Ionic basis for the electro-responsiveness and oscillatory properties of guinea-pig thalamic neurones in vitro. The Journal of physiology. 1984; 349:227–247. [PubMed: 6737293]

Jann MW, Lam YW, Chang WH. Rapid formation of clozapine in guinea-pigs and man following clozapine-N-oxide administration. Archives internationales de pharmacodynamie et de therapie. 1994; 328:243–250. [PubMed: 7710309]

Jones, EG. The thalamus. 2nd edition. Cambridge University Press; New York, N.Y.: 2007.

Jones MW, Wilson MA. Theta rhythms coordinate hippocampal-prefrontal interactions in a spatial memory task. PLoS biology. 2005; 3:e402. [PubMed: 16279838]

Kellendonk C, Simpson EH, Polan HJ, Malleret G, Vronskaya S, Winiger V, Moore H, Kandel ER. Transient and selective overexpression of dopamine D2 receptors in the striatum causes persistent abnormalities in prefrontal cortex functioning. Neuron. 2006; 49:603–615. [PubMed: 16476668]

Kuroda M, Yokofujita J, Murakami K. An ultrastructural study of the neural circuit between the prefrontal cortex and the mediodorsal nucleus of the thalamus. Progress in neurobiology. 1998; 54:417–458. [PubMed: 9522395]

Lavin A, Grace AA. Response of the ventral pallidal/mediodorsal thalamic system to antipsychotic drug administration: involvement of the prefrontal cortex. Neuropsychopharmacology. 1998; 18:352–363. [PubMed: 9536448]

Leeson VC, Robbins TW, Matheson E, Hutton SB, Ron MA, Barnes TR, Joyce EM. Discrimination learning, reversal, and set-shifting in first-episode schizophrenia: stability over six years and

specific associations with medication type and disorganization syndrome. Biological psychiatry. 2009; 66:586–593. [PubMed: 19576575]

Loffler S, Korber J, Nubbemeyer U, Fehsel K. Comment on “Impaired respiratory and body temperature control upon acute serotonergic neuron inhibition”. Science. 2012; 337:646. author reply 646. [PubMed: 22879486]

Marenco S, Stein JL, Savostyanova AA, Sambataro F, Tan HY, Goldman AL, Verchinski BA, Barnett AS, Dickinson D, Apud JA, et al. Investigation of anatomical thalamo-cortical connectivity and FMRI activation in schizophrenia. Neuropsychopharmacology. 2012; 37:499–507. [PubMed: 21956440]

McOmish CE, Lira A, Hanks JB, Gingrich JA. Clozapine-Induced Locomotor Suppression is Mediated by 5-HT(2A) Receptors in the Forebrain. Neuropsychopharmacology. 2012; 37:2747–2755. [PubMed: 22871913]

Minzenberg MJ, Laird AR, Thelen S, Carter CS, Glahn DC. Meta-analysis of 41 functional neuroimaging studies of executive function in schizophrenia. Archives of general psychiatry. 2009; 66:811–822. [PubMed: 19652121]

Mitchell AS, Dalrymple-Alford JC. Dissociable memory effects after medial thalamus lesions in the rat. The European journal of neuroscience. 2005; 22:973–985. [PubMed: 16115220]

Mitelman SA, Byne W, Kemether EM, Hazlett EA, Buchsbaum MS. Metabolic disconnection between the mediodorsal nucleus of the thalamus and cortical Brodmann's areas of the left hemisphere in schizophrenia. The American journal of psychiatry. 2005; 162:1733–1735. [PubMed: 16135634]

Neave N, Sahgal A, Aggleton JP. Lack of effect of dorsomedial thalamic lesions on automated tests of spatial memory in the rat. Behavioural brain research. 1993; 55:39–49. [PubMed: 8329125]

Pettersson-Yeo W, Allen P, Benetti S, McGuire P, Mechelli A. Dysconnectivity in schizophrenia: where are we now? Neuroscience and biobehavioral reviews. 2011; 35:1110–1124. [PubMed: 21115039]

Ray RS, Corcoran AE, Brust RD, Kim JC, Richerson GB, Nattie E, Dymecki SM. Impaired respiratory and body temperature control upon acute serotonergic neuron inhibition. Science. 2011; 333:637–642. [PubMed: 21798952]

Rolls ET, Hornak J, Wade D, McGrath J. Emotion-related learning in patients with social and emotional changes associated with frontal lobe damage. Journal of neurology, neurosurgery, and psychiatry. 1994; 57:1518–1524.

Rygula R, Walker SC, Clarke HF, Robbins TW, Roberts AC. Differential contributions of the primate ventrolateral prefrontal and orbitofrontal cortex to serial reversal learning. J Neurosci. 2010; 30:14552–14559. [PubMed: 20980613]

Schoenbaum G, Nugent SL, Saddoris MP, Setlow B. Orbitofrontal lesions in rats impair reversal but not acquisition of go, no-go odor discriminations. Neuroreport. 2002; 13:885–890. [PubMed: 11997707]

Siapas AG, Lubenov EV, Wilson MA. Prefrontal phase locking to hippocampal theta oscillations. Neuron. 2005; 46:141–151. [PubMed: 15820700]

Siegel M, Warden MR, Miller EK. Phase-dependent neuronal coding of objects in short-term memory. Proceedings of the National Academy of Sciences of the United States of America. 2009; 106:21341–21346. [PubMed: 19926847]

Sigurdsson T, Stark KL, Karayiorgou M, Gogos JA, Gordon JA. Impaired hippocampal-prefrontal synchrony in a genetic mouse model of schizophrenia. Nature. 2010; 464:763–767. [PubMed: 20360742]

Simpson EH, Kellendonk C, Kandel E. A possible role for the striatum in the pathogenesis of the cognitive symptoms of schizophrenia. Neuron. 2010; 65:585–596. [PubMed: 20223196]

Tallon-Baudry C, Bertrand O, Fischer C. Oscillatory synchrony between human extrastriate areas during visual short-term memory maintenance. J Neurosci. 2001; 21:RC177. [PubMed: 11588207]

Tallon-Baudry C, Mandon S, Freiwald WA, Kreiter AK. Oscillatory synchrony in the monkey temporal lobe correlates with performance in a visual short-term memory task. Cereb Cortex. 2004; 14:713–720. [PubMed: 15054050]

Uhlhaas PJ, Singer W. Abnormal neural oscillations and synchrony in schizophrenia. Nature reviews. 2010; 11:100–113.

Vinck M, Battaglia FP, Womelsdorf T, Pennartz C. Improved measures of phase-coupling between spikes and the Local Field Potential. Journal of computational neuroscience. 2012; 33:53–75. [PubMed: 22187161]

Watanabe Y, Funahashi S. Thalamic mediodorsal nucleus and working memory. Neuroscience and biobehavioral reviews. 2012; 36:134–142. [PubMed: 21605592]

Weinberger DR, Berman KF. Prefrontal function in schizophrenia: confounds and controversies. Philosophical transactions of the Royal Society of London. 1996; 351:1495–1503. [PubMed: 8941961]

Woodward ND, Karbasforoushan H, Heckers S. Thalamocortical dysconnectivity in schizophrenia. The American journal of psychiatry. 2012; 169:1092–1099. [PubMed: 23032387]

Yoon T, Okada J, Jung MW, Kim JJ. Prefrontal cortex and hippocampus subserve different components of working memory in rats. Learning & memory. 2008; 15:97–105. [PubMed: 18285468]

Highlights

1. A mild decrease in MD activity triggers impairments in PFC-dependent cognitive tasks.
2. MD-PFC beta-synchrony is selectively modulated during a spatial working memory task.
3. Decreasing MD activity disrupts MD-PFC synchrony during high working memory demand.
4. Decreasing MD activity delays task acquisition and correlated increases in synchrony.

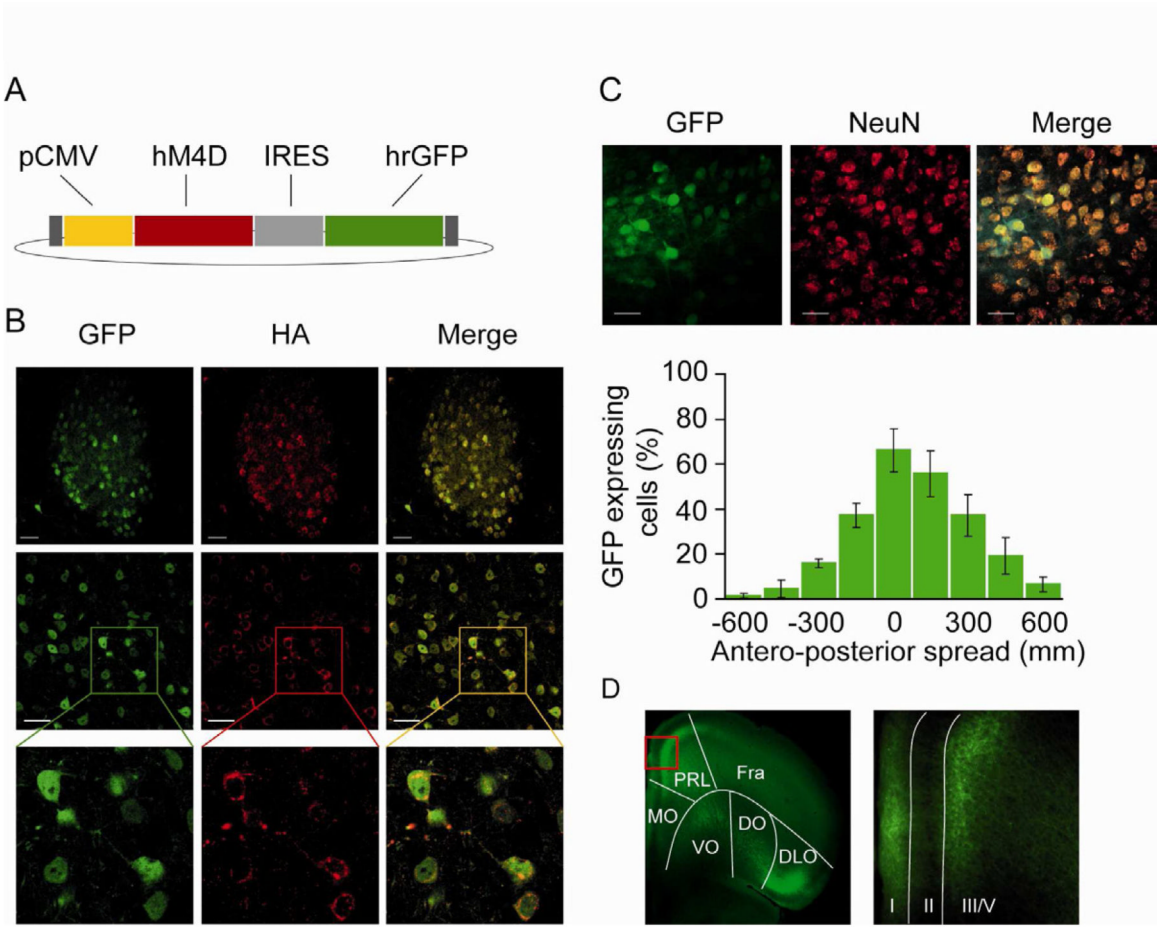

Figure 1. Expression of hM4D in the medio-dorsal thalamus using viral vector

(A) Schematic drawing of pAAV2-hM4D-IRES-hrGFP plasmid. Both hM4D (red) and hrGFP (green) are expressed under the control of a cytomegalovirus (CMV) promoter (yellow). **(B)** Native hrGFP fluorescence (green) and anti-HA immunostaining (red) reveal co-expression (yellow) of GFP and hM4D in MD cells. **(C)** Top panel: native hrGFP and anti-NeuN immunostaining (red) reveal that hrGFP is exclusively expressed in neurons. Bottom panel: stereotactic injection of the AAV2-hM4D-IRES-hrGFP leads to transgene expression in 27 ±6% of MD neurons with a peak at 66 ±9.6% at the site of infection (n=4). **(D)** GFP labels the MD projections to the PFC after injection with a hrGFP control virus in the MD. Abbreviations: prelimbic (PrL), medial ventral orbital (VO), lateral orbital (LO) dorsolateral orbital (DLO) cortices, I, III/V depict cortical layers. See also figure S1.

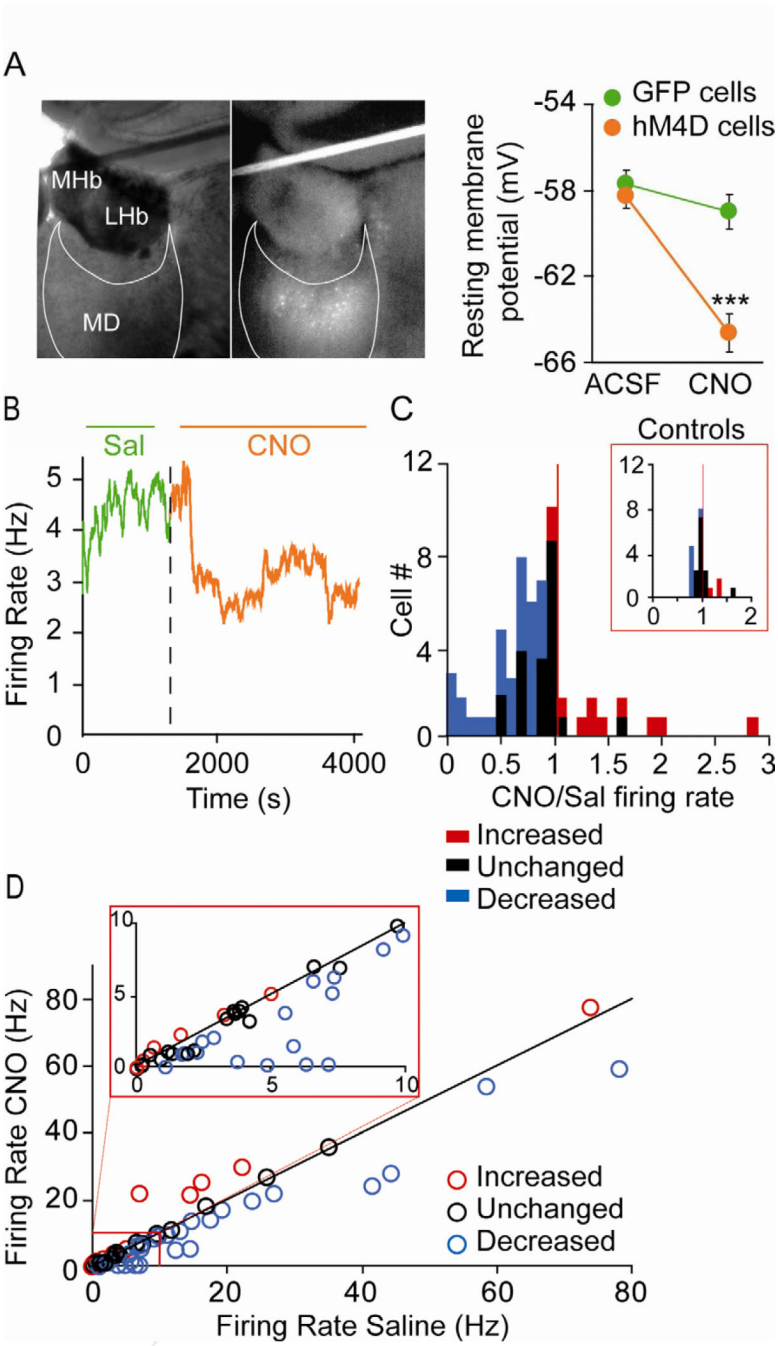

Figure 2. Decreasing activity in the medio-dorsal thalamus using a pharmaco-genetic approach

(A) Left panel: visualization of hM4D ires hrGFP expressing neurons in a thalamic slice. Right panel: Resting membrane potential of MD neurons infected with control hrGFP (green) and experimental hM4D ires hrGFP (orange) virus before and after bath application of 1 μM CNO (repeated measures ANOVA, group x treatment interaction ***$p<0.001$; n=11 and 10 cells for hrGFP and hM4D-hrGFP cells). **(B)** Example of MD unit activity *in vivo* before (green) and after (orange) systemic injection of 2 mg/kg CNO to anMD_{hM4D} mouse. **(C)** Histogram of the ratios of firing rate after CNO to firing rate after saline in MD_{hM4D} mice. Red and blue bars represent cells with statistically significant increases or

decreases in firing rate, respectively. Inset: histogram of the ratios of firing rate after CNO to firing rate after saline in wild-type mice. **(D)** Firing rate after saline vs. firing rate after CNO for entire sample of 63 MD units. Red and blue circles indicate units with statistically significant increases or decreases in firing rate, respectively ($p<0.05$, paired t-test). Inset is a magnified view of lower firing-rate neurons. Error bars: s.e.m.See also figure S2.

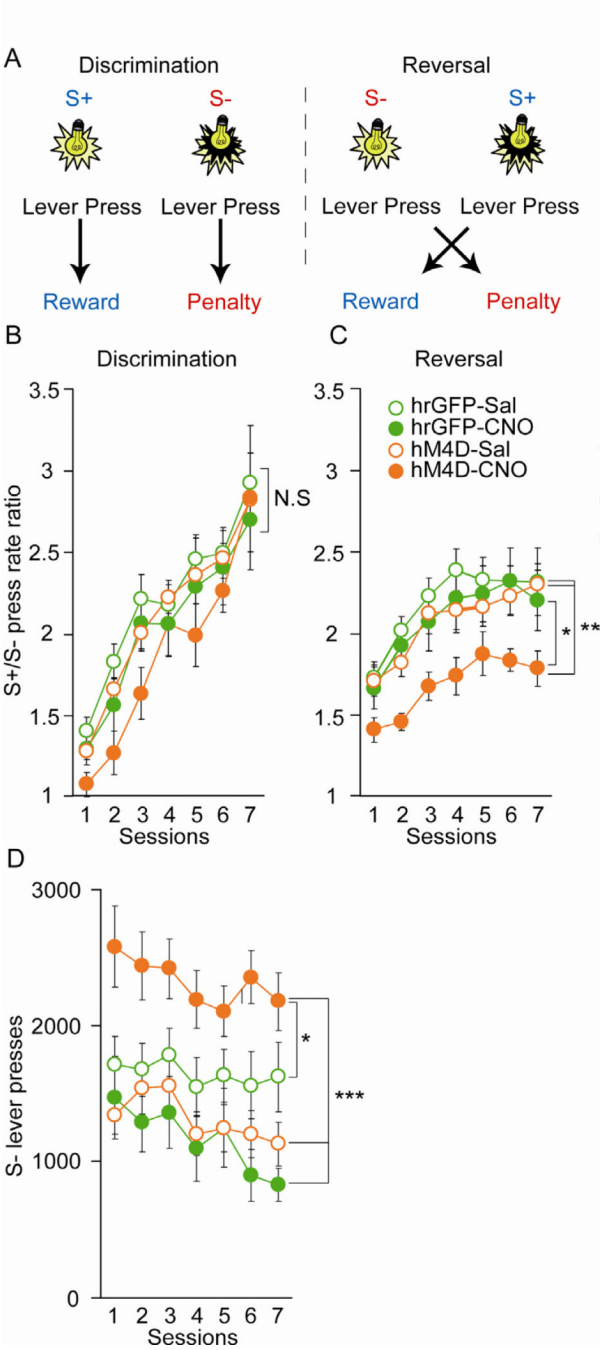

Figure 3. Decreasing activity in the medio-dorsal thalamus leads to deficits in behavioral flexibility

(A) Task design for the operant-based reversal-learning task. **(B and C)** Acquisition curves for discrimination (B) and reversal (C) demonstrate a selective impairment in reversal learning in CNO-treated MD_{hM4D} mice. (Discrimination: repeated measures ANOVA, time $p<0.001$, group $p=0.3593$; GFP-sal n=23, GFP-CNO n=7, hM4D-sal n=42 and hM4D-CNO n=11; Reversal; repeated measures ANOVA followed by Bonferroni post-hoc tests, $*p<0.05$, $**p<0.01$; GFP-sal n=15, GFP-CNO n=14, hM4D-sal n=26 and hM4D-CNO n=25). **(D)** S- lever pressing during the reversal phase. All mice decreased responding over time (repeated measures ANOVA, main effect of time, $p<0.001$). However, only CNO-

treated MD_{hM4D} mice made more perseverative errors (repeated measures ANOVA followed by Bonferroni post-hoc analysis *p<0.05, ***p<0.001). Error bars: s.e.m. See also Figure S3.

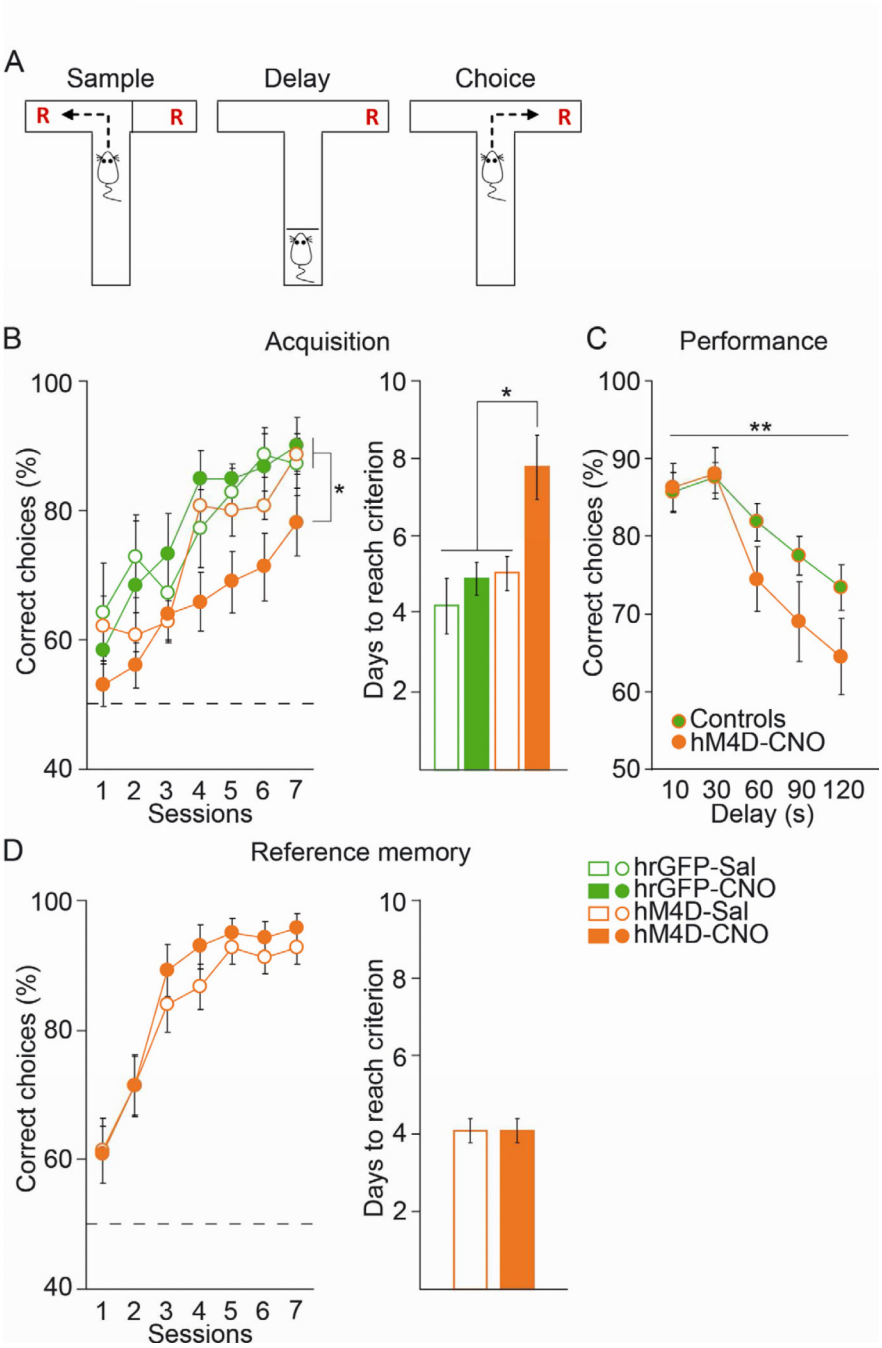

Figure 4. Decreasing activity in the medio-dorsal thalamus leads to deficits in working memory

(A) Task design for the T-maze based DNMS working memory task. **(B)** CNO-treated MD_{hM4D} mice showed a deficit in acquisition (left panel) and took longer to reach criterion (right panel) compared to control groups (delayed task) (ANOVA followed by Newman-Keuls post-hoc analysis *p<0.05; GFP-sal n=7 GFP-CNO n=6, hM4D-sal n=12 and hM4D-CNO n=11). **(C)** CNO-treatment impaired DNMS performance on long delays in MD_{hM4D} mice after task acquisition (repeated measures ANOVA, group effect *p<0.05; combined controls n=21 including 5 GFP-sal, 4 GFP-CNO and 12 hM4D-sal; hM4D-CNO n=11). **(D)** Decreasing MD activity does not affect acquisition of a spatial reference memory T-maze

task (two-tailed t-test p=0.98; hM4D-sal n=15 and hM4D-CNO n=14). Error bars: s.e.m. See also figure S4.

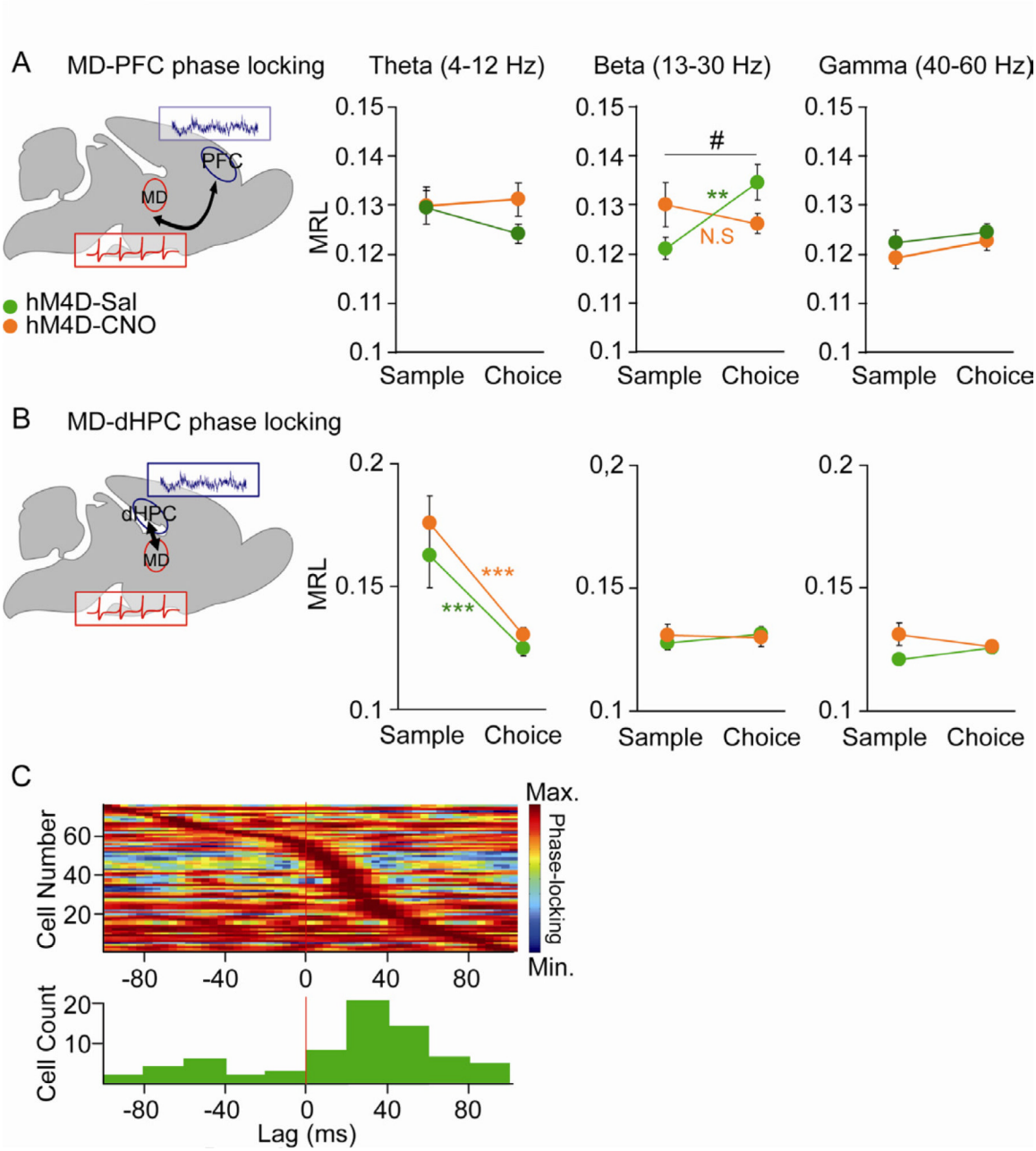

Figure 5. Enhancement of thalamo-prefrontal beta synchrony during working memory performance is disrupted by low MD activity

(A) Phase locking of MD cells to mPFC LFP oscillations in the beta-, theta- and gamma-frequency range as a function of task phase (sample vs choice) (repeated measures ANOVA, group x task phase interaction #p<0.05; hM4D-SAL cells n=40 (green), hM4D-CNO cells n=33 (orange); sample-choice difference in controls, **p < 0.01 by paired t-test). **(B)** Phase locking of MD cells to dHPC LFP oscillations in the beta-, theta- and gamma-frequency range as a function of task phase (sample vs choice) (paired t-test sample-choice difference in controls and CNO-treated MD_{hM4D} mice, ***p < 0.001; hM4D-SAL cells n=40 (green), hM4D-CNO cells n=33 (orange)). **(C)** Upper panel, normalized beta-phase locking strength as a function of lag to mPFC LFP for all MD cells with significant phase-locking to the mPFC, ordered by lag at which peak strength occurs. Bottom: distribution of lags at peak

phase locking strength (lag, +20 ± 1.4 ms, wilcoxon signed rank test $p<0.05$, n=73). Error bars: s.e.m. See also Figure S5.

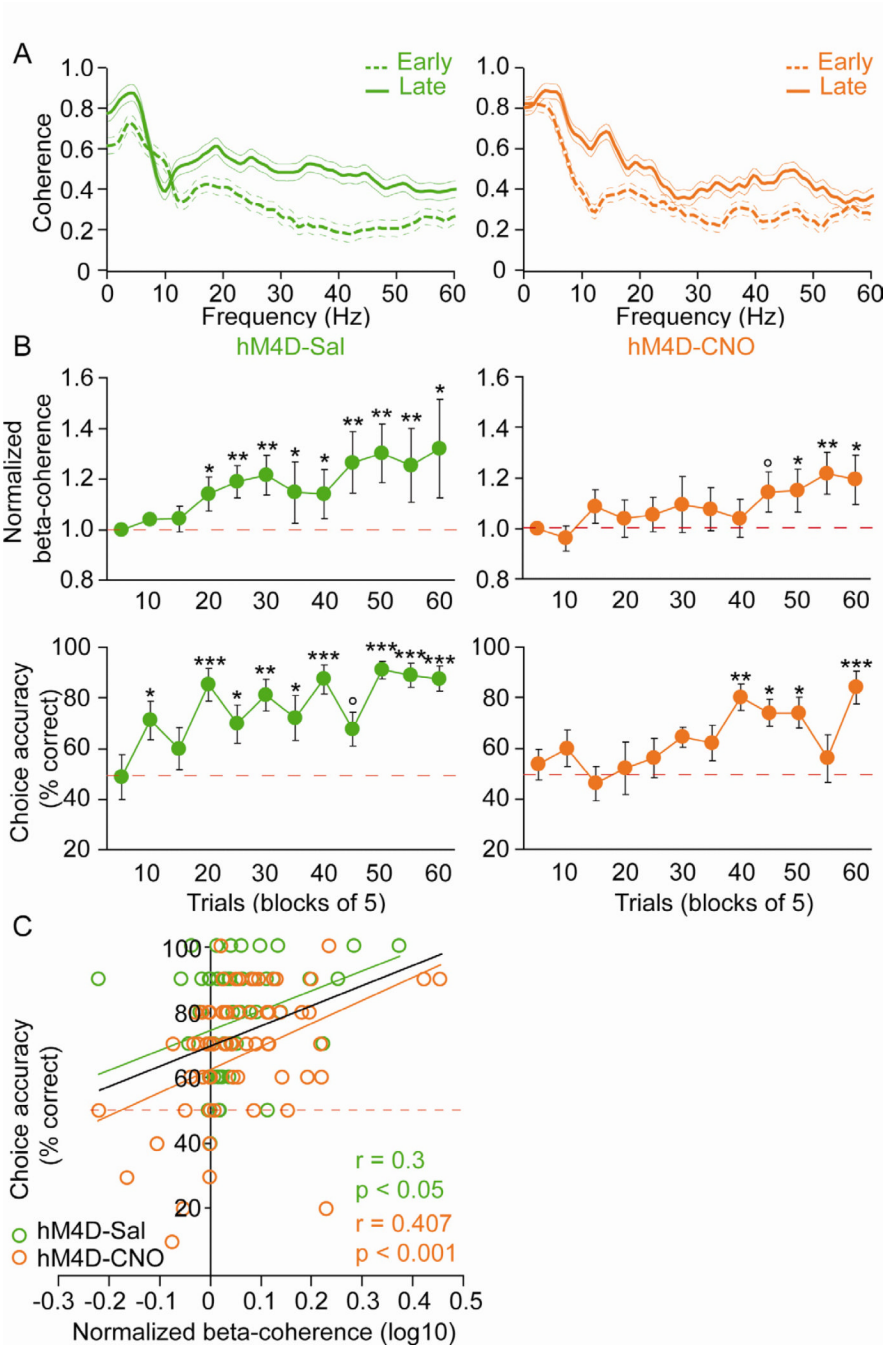

Figure 6. Synchronous activity between medio-dorsal thalamus and prefrontal cortex correlates with behavioral performance in a spatial working memory task

(A) Example of coherence spectra between early (trials 1-5; dashed lines) and late (5 last trials; solid lines) training phase in saline- (green) and CNO- (orange) treated MD_{hM4D} mice. **(B)** Time course of increases in MD-PFC beta coherence (top panels) and choice accuracy (bottom panels) in saline- (green, n=9) and a CNO- (orange, n=10) treated MD_{hM4D} mice (repeated measures ANOVA followed by Fischer post-hoc analysis, difference versus trials 1-5, °p<0.1 *p<0.05, **p<0.01, ***p<0.001). **(C)** Correlation analysis between beta-coherence and choice accuracy for each session (10 trials per session) in saline- (green) and CNO- (orange) treated MD_{hM4D} mice (Pearson correlation test, saline:

correlation coefficient r=0.3, p<0.05, CNO: r=0.407, p<0.001). Error bars: s.e.m. See also Figure S6.